J. KSIAM Vol.14, No.2, 67–78, 2010

NUMERICAL ANALYSIS OF A LAMINATED COMPOSITE ELASTIC FIELD WITH ROLLER GUIDED PANEL

JAEGWI GO† AND MOHAMED AFSAR ALI

DEPARTMENT OF MATHEMATICS, CHANGWON NATIONAL UNIVERSITY, SOUTH KOREA
E-mail address: jagwigo@changwon.ac.kr

SCHOOL OF MECHATRONICS, CHANGWON NATIONAL UNIVERSITY, SOUTH KOREA
E-mail address: mdafsarali1967@yahoo.com

ABSTRACT. An elastic field composed of symmetric cross-ply laminated material is analyzed in roller guided panel. The plane stress elasticity problem is formulated in terms of two displacement parameters with mixed boundary conditions. The numerical solution for two displacement parameters is obtained using a finite element method considering a panel of glass/epoxy laminated composite. Some components of stress and displacement at different sections of panel are displayed. The results makes sure that the formulation developed in this study can be applied to analyze the characteristics of elastic field made of laminated composite under any boundary conditions.

1. INTRODUCTION

In structural elements composite materials presents better performance in engineering applications in comparison with conventional materials. But, most of previous results were obtained when structural elements are under the action of loads or constraints along their boundaries, while many kind of structural elements, in general, experience both loads and constraints at the same time. Thus, the materials of the elements suffer from displacement and stress, which provides the necessity to investigate the elastic characteristics of the materials for reliable performance in an application.

Chow *et al.* [4] used the Airy stress function formulation for two dimensional elastic problem. Effective solution for the derived equation were obtained based on the finite difference technique. The Airy stress function formulation was developed into a Fourier Integrals form by Conway and Ithaca [5] for orthotropic materials. Timoshenko and Goodier [8] extended the Airy stress function approach into the plane boundary value elastic problem for the mathematical modelling. But, the stress function approach is valid for the loading boundary value problem only.

Received by the editors February 18 2010; Revised March 23 2010; Accepted in revised form March 24 2010.
2000 *Mathematics Subject Classification.* 74B99.
Key words and phrases. Elasticity, Panel, Symmetric Laminated Composite.
† Corresponding author.

Meanwhile, the displacement formulations was mentioned by Uddin [9] for the elastic field problems. Two second order partial differential equations are derived for equilibrium involving two displacement parameters in this approach. But, it is hard work to solve two second order partial differential equations simultaneously. Ahmed *et al.* [3] thus developed the displacement approach for the isotropic elasticity problem with mixed boundary conditions in attempting to find analytical solution. Due to the outstanding advantage that the approach can be applicable to any boundary conditions prescribed in terms of either stress or displacement or mixed type, the displacement approach for the isotropic elasticity problem with mixed boundary conditions in attempting to find analytical solution. Due to the outstanding advantage that the approach can be applicable to any boundary conditions prescribed in terms of either stress or displacement or mixed type, the displacement approach has been extended by many authors such as Nath, Afsar, and Ahmed [2, 6–7] for orthotropic composite material problems.

The characteristics of a symmetric cross-ply laminated composite field guided by roller panel is investigated in the present study. The elastic field is subjecting to mixed boundary conditions. The displacement approach is applied to the laminated composite field problem, which provides two second order partial differential equations involving two displacement parameters. The mixed boundary condition is formulated in terms of displacement potential functions. The govern equations are discretized using a finite element method and solved for two displacement parameters simultaneously. The two displacements obtained are used for other stresses and displacements, since all the components of stress and displacements are expressed in terms of the solution. The results may be applicable to sliding door and window, sliding fences, and sliding sun roofs.

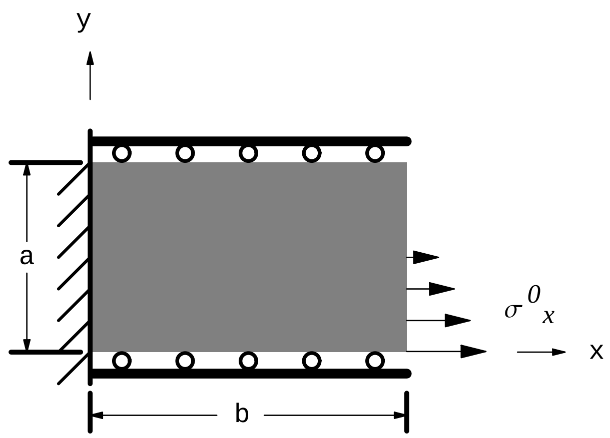

FIGURE 1. A rectangle roller guided panel

2. Mathematical Modelling

2.1. **Mathematical formulation.** A rectangular panel of symmetric cross-ply laminated composite is considered in two dimensional Cartesian frame (See Fig. 1). a and b represent the width and length of the panel, respectively. The left lateral side of the panel is constraint along the y-axis and the two longitudinal sides parallel to the x-axis are roller guided. We assume that no shear stress appears on roller guided sides and no displacement on edges perpendicular to roller guided sides. In addition, the right side of panel is assumed to be subjected to a linearly varying tensile load $\sigma_x^0 = P(1-2y/a)$, where P is the maximum value of the load. The governing equations are derived founded on the concept of the displacement potential approach established for an orthotropic lamina [6–7].

Under the following facts: (i) the bending-extension coupling stiffness matrix vanishes [10] and the strains of mid plane equals to the global strains, when a symmetric laminate is pressured with a in-plane loading, (ii) the values of shear-extension coupling terms of the extensional stiffness matrix are zero, the average stress-strain relations for such a laminate under plane stress in global coordinates system can be formulated as

$$\begin{bmatrix}\sigma_x\\ \sigma_y\\ \tau_{xy}\end{bmatrix} = \frac{1}{h}\begin{bmatrix}A_{11} & A_{12} & 0\\ A_{12} & A_{22} & 0\\ 0 & 0 & A_{66}\end{bmatrix}\begin{bmatrix}\varepsilon_x\\ \varepsilon_y\\ \gamma_{xy}\end{bmatrix}$$

where σ_x and σ_y are normal stress components in the x- and y- directions, respectively, τ_{xy} the shear stress component, ε_x and ε_y normal strain components in the x- and y- directions, respectively, γ_{xy} the shear strain component. The elements of stiffness matrix $[A]$ are given by

$$\begin{aligned}
A_{11} &= \sum_{k=1}^{n}[Q_{11}\cos^4\theta + Q_{22}\sin^4\theta + 2(Q_{12}+2Q_{66})\cos^2\theta\sin^2\theta]_k(h_k-h_{k-1})\\
A_{12} &= \sum_{k=1}^{n}[(Q_{11}+Q_{22}-4Q_{66})\cos^2\theta\sin^2\theta + Q_{12}(\cos^4\theta+\sin^4\theta)]_k(h_k-h_{k-1})\\
A_{22} &= \sum_{k=1}^{n}[Q_{11}\sin^4\theta + Q_{22}\cos^4\theta + 2(Q_{12}+2Q_{66})\cos^2\theta\sin^2\theta)]_k(h_k-h_{k-1})\\
A_{66} &= \sum_{k=1}^{n}[(Q_{11}+Q_{22}-2Q_{12}-2Q_{66})\cos^2\theta\sin^2\theta + Q_{66}(\cos^4\theta+\sin^4\theta)]_k(h_k-h_{k-1}),
\end{aligned}$$

where $Q_{11} = \dfrac{E_1}{1-\nu_{21}\nu_{12}}$, $Q_{12} = \dfrac{\nu_{12}E_2}{1-\nu_{21}\nu_{12}}$, $Q_{22} = \dfrac{E_2}{1-\nu_{21}\nu_{12}}$, $Q_{66} = G_{12}$, $h_k - h_{k-1}$ is the thickness of the k-th ply of the laminate, h the total thickness of the laminate, θ the angle between the x-axis and the fiber direction of a lamina in the laminate, E_1 and E_2 the Young's modulus in the longitudinal and transverse directions, respectively, ν_{12} and ν_{21} the major and minor Poison's ratio, respectively, and G_{12} the in-plane shear modulus of a lamina in the laminate. From the basic strain-displacement relations, the above matrix form equations can be rewritten by

$$\begin{aligned}
\sigma_x &= \frac{1}{h}[A_{11}\frac{\partial u_x}{\partial x} + A_{12}\frac{\partial u_y}{\partial y}] \\
\sigma_y &= \frac{1}{h}[A_{21}\frac{\partial u_x}{\partial x} + A_{22}\frac{\partial u_y}{\partial y}] \\
\tau_{xy} &= \frac{1}{h}[A_{66}\frac{\partial u_x}{\partial y} + A_{66}\frac{\partial u_y}{\partial x}],
\end{aligned} \tag{2.1}$$

where u_x and u_y are two displacement components in the x- and y-direction, respectively.

The equilibrium equation for the plane elasticity problems without any body force are given by

$$\begin{aligned}
\frac{\partial \sigma_x}{\partial x} + \frac{\partial \tau_{xy}}{\partial y} &= 0 \\
\frac{\partial \sigma_y}{\partial y} + \frac{\partial \tau_{xy}}{\partial x} &= 0.
\end{aligned} \tag{2.2}$$

Combination of (2.1) and (2.2) provides

$$\begin{aligned}
A_{11}\frac{\partial^2 u_x}{\partial x^2} + (A_{12} + A_{66})\frac{\partial^2 u_y}{\partial x \partial y} + A_{66}\frac{\partial^2 u_x}{\partial y^2} &= 0 \\
A_{66}\frac{\partial^2 u_y}{\partial x^2} + (A_{12} + A_{66})\frac{\partial^2 u_x}{\partial x \partial y} + A_{22}\frac{\partial^2 u_y}{\partial y^2} &= 0.
\end{aligned} \tag{2.3}$$

The boundary conditions for the present roller guided panel shown in Fig. 1 are

$$\begin{aligned}
u_x(0, y) = u_y(0, y) = 0, &\quad 0 \le y \le a \\
u_y(x, 0) = u_y(x, a) = 0, &\quad 0 \le x \le b \\
\sigma_{xy}(x, 0) = \sigma_{xy}(x, a) = 0, &\quad 0 \le x \le b \\
\sigma_{xy}(b, y) = 0, &\quad 0 \le y \le a \\
\sigma_x(b, y) = P(1 - \tfrac{2y}{a}), &\quad 0 \le y \le \frac{a}{2}.
\end{aligned}$$

2.2. **Variational formulation.** The governing equations (2.3) can be expressed in terms of

$$\begin{aligned}
\frac{\partial}{\partial x}(A_{11}\frac{\partial u_x}{\partial x} + A_{12}\frac{\partial u_y}{\partial y}) + \frac{\partial}{\partial y}(A_{66}\frac{\partial u_x}{\partial y} + A_{66}\frac{\partial u_y}{\partial x}) &= 0 \\
\frac{\partial}{\partial x}(A_{66}\frac{\partial u_y}{\partial x} + A_{66}\frac{\partial u_x}{\partial y}) + \frac{\partial}{\partial y}(A_{12}\frac{\partial u_x}{\partial x} + A_{22}\frac{\partial u_y}{\partial y}) &= 0.
\end{aligned}$$

The boundary stress components can also be expressed in terms of the displacements:

$$\begin{aligned}
t_x &= n_x(A_{11}\frac{\partial u_x}{\partial x} + A_{12}\frac{\partial u_y}{\partial y}) + n_y(A_{66}\frac{\partial u_x}{\partial y} + A_{66}\frac{\partial u_y}{\partial x}) \\
t_y &= n_x(A_{66}\frac{\partial u_y}{\partial x} + A_{66}\frac{\partial u_x}{\partial y}) + n_y(A_{12}\frac{\partial u_x}{\partial x} + A_{22}\frac{\partial u_y}{\partial y}).
\end{aligned} \tag{2.4}$$

Multiplying the first equation with a weight function w_1 and the second equation with a weight function w_2, and integrating by parts to trade the differentiation equally between the weight function and the dependent variables provide

$$\int_{\Omega^e}[\frac{\partial w_1}{\partial x}(A_{11}\frac{\partial u_x}{\partial x}+A_{12}\frac{\partial u_y}{\partial y})+\frac{\partial w_1}{\partial y}(A_{66}\frac{\partial u_x}{\partial y}+A_{66}\frac{\partial u_y}{\partial x})]dxdy=-\oint_{\Gamma^e}w_1t_xds$$

$$\int_{\Omega^e}[\frac{\partial w_2}{\partial x}(A_{66}\frac{\partial u_y}{\partial x}+A_{66}\frac{\partial u_x}{\partial y})+\frac{\partial w_2}{\partial y}(A_{12}\frac{\partial u_x}{\partial x}+A_{22}\frac{\partial u_y}{\partial y})]dxdy=-\oint_{\Gamma^e}w_2t_yds. \quad (2.5)$$

The equation (2.5) can be expressed as

$$B^{11}(w_1,u_x)+B^{12}(w_1,u_y)=l^1(w_1)$$

$$B^{21}(w_2,u_x)+B^{22}(w_2,u_y)=l^2(w_2), \quad (2.6)$$

where the bilinear and linear functions can be written by comparison to equations (2.5).

Let u and v be approximated over Ω^e by the finite element interpolations

$$u_x \approx \sum_{j=1}^{n}u_j^{(e)}\phi_j^{(e)}$$

$$u_y \approx \sum_{j=1}^{n}v_j^{(e)}\phi_j^{(e)}, \quad (2.7)$$

where $u_j^{(e)}$ and $v_j^{(e)}$ are the nodal values of the primary variables. Using the Ritz method, we write

$$\sum_{j=1}^{n}B^{11}(\phi_i^{(e)},\phi_j^{(e)})u_j^{(e)}+\sum_{j=1}^{n}B^{12}(\phi_i^{(e)},\phi_j^{(e)})v_j^{(e)}=l^1(\phi_i^{(e)})$$

$$\sum_{j=1}^{n}B^{21}(\phi_i^{(e)},\phi_j^{(e)})u_j^{(e)}+\sum_{j=1}^{n}B^{22}(\phi_i^{(e)},\phi_j^{(e)})v_j^{(e)}=l^2(\phi_i^{(e)}) \quad (2.8)$$

or

$$[K^{11(e)}]\{u^{(e)}\}+[K^{12(e)}]\{v^{(e)}\}=\{F^{1(e)}\}$$

$$[K^{21(e)}]\{u^{(e)}\}+[K^{22(e)}]\{v^{(e)}\}=\{F^{2(e)}\}, \quad (2.9)$$

where

$$K_{ij}^{11(e)}=\int_{\Omega^e}[A_{11}\frac{\partial\phi_i^{(e)}}{\partial x}\frac{\partial\phi_j^{(e)}}{\partial x}+A_{66}\frac{\partial\phi_i^{(e)}}{\partial y}\frac{\partial\phi_j^{(e)}}{\partial y}]dxdy$$

$$\begin{aligned} K_{ij}^{12(e)} &= K_{ji}^{21(e)} \\ &= \int_{\Omega^e} [A_{12} \frac{\partial \phi_i^{(e)}}{\partial x} \frac{\partial \phi_j^{(e)}}{\partial y} + A_{66} \frac{\partial \phi_i^{(e)}}{\partial y} \frac{\partial \phi_j^{(e)}}{\partial x}] dxdy \end{aligned}$$

$$K_{ij}^{22(e)} = \int_{\Omega^e} [A_{66} \frac{\partial \phi_i^{(e)}}{\partial x} \frac{\partial \phi_j^{(e)}}{\partial x} + A_{22} \frac{\partial \phi_i^{(e)}}{\partial y} \frac{\partial \phi_j^{(e)}}{\partial y}] dxdy$$

$$F_i^{1(e)} = -\oint_{\Gamma^e} t_x \phi_i^{(e)} ds$$

$$F_i^{2(e)} = -\oint_{\Gamma^e} t_y \phi_i^{(e)} ds. \tag{2.10}$$

Equations (2.9) can be rewritten in the form

$$\begin{bmatrix} K^{11^{(e)}} & K^{12^{(e)}} \\ K^{21^{(e)}} & K^{22^{(e)}} \end{bmatrix} \begin{Bmatrix} u^{(e)} \\ v^{(e)} \end{Bmatrix} = \begin{Bmatrix} F^{1^{(e)}} \\ F^{2^{(e)}} \end{Bmatrix},$$

and rearrange this system to get

$$[K^{(e)}]\{\Delta^{(e)}\} = \{F^{(e)}\}, \tag{2.11}$$

where

$$\{\Delta^{(e)}\}^T = \{u_1^{(e)}, v_1^{(e)}, u_2^{(e)}, v_2^{(e)}, \cdots, u_n^{(e)}, v_n^{(e)}\} \tag{2.12}$$

$$\{F^{(e)}\}^T = \{F_1^{1(e)}, F_1^{2(e)}, F_2^{1(e)}, F_2^{2(e)}, \cdots, F_n^{1(e)}, F_n^{2(e)}\}. \tag{2.13}$$

For four-node rectangular element (see Figs 2), the interpolation equations below are adopted

$$\phi_1^{(e)} = (1 - \frac{\bar{x}}{b_e})(1 - \frac{\bar{y}}{a_e})$$

$$\phi_2^{(e)} = \frac{\bar{x}}{b_e}(1 - \frac{\bar{y}}{a_e})$$

$$\phi_3^{(e)} = \frac{\bar{x}}{b_e} \frac{\bar{y}}{a_e}$$

$$\phi_4^{(e)} = (1 - \frac{\bar{x}}{b_e}) \frac{\bar{y}}{a_e},$$

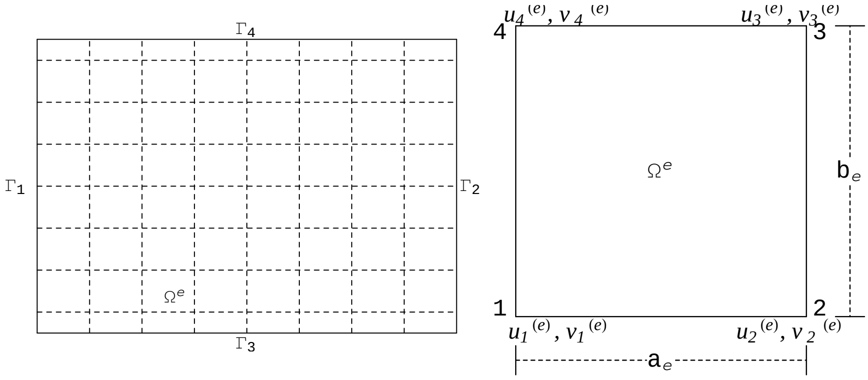

FIGURE 2. (a) Discretization of domain and (b) Four-node element

and thus, after dropping the (e) superscript, we obtain

$$[K^e] = \begin{pmatrix} K_{11}^{11} & K_{11}^{12} & K_{12}^{11} & K_{12}^{12} & K_{13}^{11} & K_{13}^{12} & K_{14}^{11} & K_{14}^{12} \\ & K_{11}^{22} & K_{12}^{21} & K_{12}^{22} & K_{13}^{21} & K_{13}^{22} & K_{14}^{21} & K_{14}^{22} \\ & & K_{22}^{11} & K_{22}^{12} & K_{23}^{11} & K_{23}^{12} & K_{24}^{11} & K_{24}^{12} \\ & & & K_{22}^{22} & K_{23}^{21} & K_{23}^{22} & K_{24}^{21} & K_{24}^{22} \\ & & & & K_{33}^{11} & K_{33}^{12} & K_{34}^{11} & K_{34}^{12} \\ & & symmetric & & & K_{33}^{22} & K_{34}^{21} & K_{34}^{22} \\ & & & & & & K_{44}^{11} & K_{44}^{12} \\ & & & & & & & K_{44}^{22} \end{pmatrix}.$$

3. RESULTS AND DISCUSSIONS

A panel of glass/epoxy laminated composite material is chosen for numerical study. The mechanical properties of unidirectional glopss/epoxy lamina are displayed in Table 1. The laminate is piled up with three ply ($n = 3$) in sequence [0/90/0]. Each ply has 1.0mm thickness. The applied pressure $P = 1000$MPa is taken as the maximum value. All numerical results are displayed to normalized position y/a at different sections $x/b = 0.0$, $x/b = 0.5$, $x/b = 0.9$, and $x/b = 2.9/3$. Even though we consider a laminate piled up with only three ply, the displacement approach developed can be applicable to laminate piled symmetrically up with any number of ply.

Parameters	E_1(MPa)	E_2(MPa)	G_{12}(MPa)	ν_{12}	ν_{21}
Value	38.6×10^3	8.27×10^3	4.14×10^3	0.26	0.06

TABLE 1. Mechanical properties of glass/epoxy composite

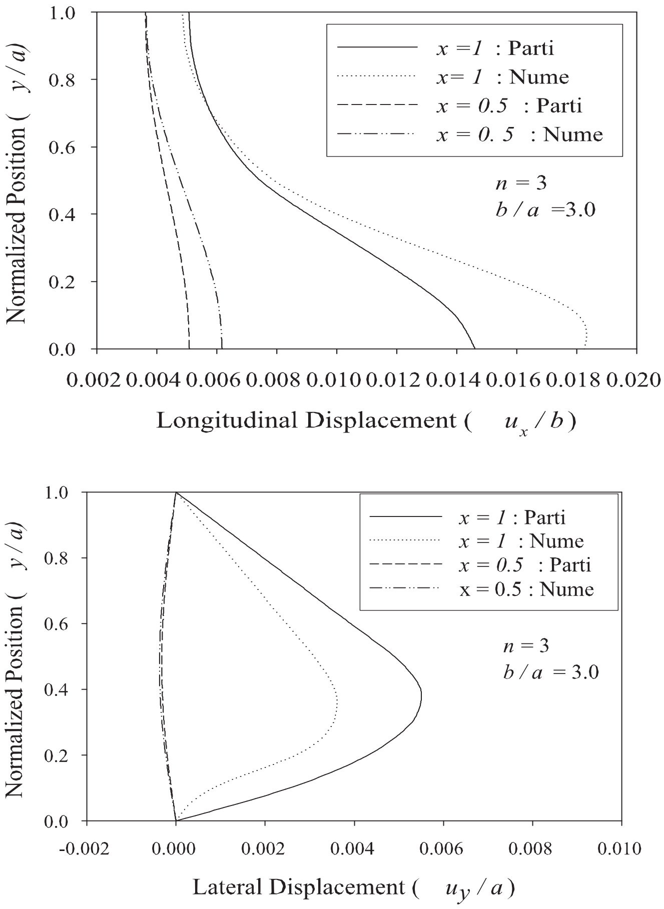

FIGURE 3. (a) Longitudinal displacement at different sections of the panel
(b) Lateral displacement at different sections of the panel

The normalized longitudinal displacement components u_x/b are presented to normalized position y/a in Fig.2-(a) corresponding to the aspect ration of the panel $b/a = 3.0$. The step sizes 0.1 and 0.05 of, respectively, normalized length and width are chosen for numerical solutions which are obtained using MATHEMATICA 5.1. The result of the present finite element model is compared with a particular solution [1] for the same problem as shown in Figs 3. As all the parameters of interest, namely stresses are computed from displacements u_x and u_y, the convergence of displacements ensures the convergence of the stresses. It is observed from Figs. 3 that the obtained shapes of solutions using the finite element model agree well with the analytical results obtained by Afsar *et al.*. The maximum difference of longitudinal displacement between the present finite element and particular solution takes place in the case of the displacement at the corner of boundary and particular solutions were underestimated

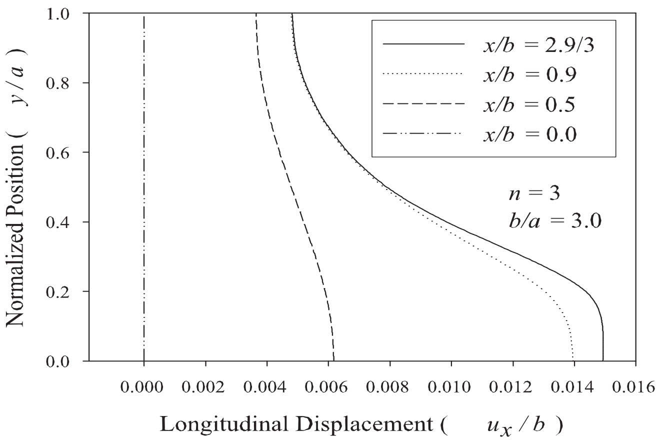

FIGURE 4. Longitudinal displacement at different sections of the panel

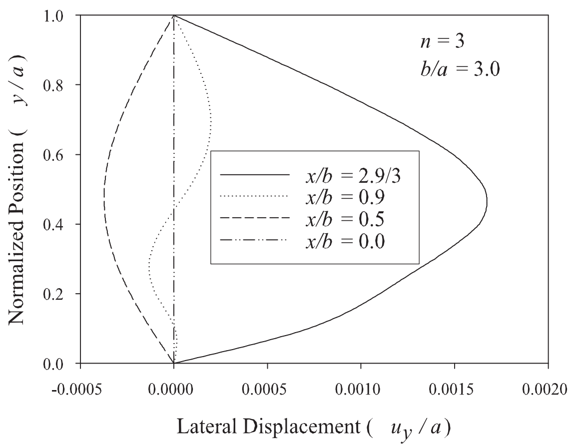

FIGURE 5. Lateral displacement at different sections of the panel

over all area (see Fig. 3-(a)). Similarly, maximum difference of lateral displacement occurs on the boundary. But, particular solution overestimated the lateral displacement over all area (see 3-(b)).

The maximum magnitude of displacement appears at the section $x/b = 2.9/3$ among the chosen sections, since external load is applied on the right lateral side (see Figs. 4, 5). The displacement decreases as the value x/b approaches to zero, and at the section $x/b = 0.0$ the magnitude of longitudinal displacement is zero which satisfies the physical boundary condition as shown Fig. 4. The maximum magnitude of longitudinal displacement of each chosen section

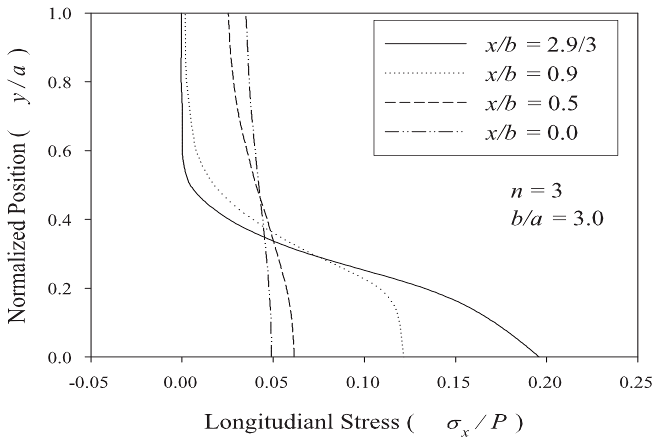

FIGURE 6. Longitudinal stress at different sections of the panel

occurs at $y/a = 0.0$ and the magnitude decreases as the value y/a approaches to 1, which agrees with the nature of the applied load distribution. Fig. 5 displays the normalized lateral displacement components u_y/b to normalized position y/a corresponding to the aspect ration of the panel $b/a = 3.0$. The figure shows that lateral displacement is zero at the bottom and top sides ($y/a = 0.0$ and $y/a = 1.0$), and left lateral edge ($x/b = 0.0$). At sections $x/b = 2.9/3$ and $x/b = 0.5$ the displacement develops to one direction while at sections $x/b = 0.9$ the displacement occurs to two directions. The maximum displacement appears at a value around $y/a = 0.5$ for sections $x/b = 2.9/3$ and $x/b = 0.5$ which justifies the physical state of the problem, but, the displacement is zero at the value at the section $x/b = 0.9$.

Fig. 6 exhibits the distribution of normalized longitudinal stress component σ_x/P to normalized position y/a. The aspect ratio of the panel is $b/a = 3.0$. The results at the section $x/b = 1.0$ agree with the applied load, and all distribution decrease as x/b approaches to zero. Through the results in Fig. 6 the Saint Venant's principle is verified. The maximum magnitude of lateral stress, unlike the longitudinal stress component, does not occur at the value $y/a = 0.0$. The sections $x/b = 2.9/3$ and $x/b = 0.9$ have the maximum stress at $y/a = 0.0$, but the section $x/b = 0.5$ has the the maximum stress at $y/a = 1.0$ (see Fig. 7). However, the lateral stress components except boundary and sections nearly close to the boundary are insignificant, since the components display about 60% of the applied load.

The normalized shear stress σ_{xy}/P components are presented in Fig. 8 as a function y/a. At all sections the values of shear stress are zero when $y/a = 0.0$ and $y/a = 1.0$. Based on the physical condition we estimate easily the shear stress, which displays zero on the right lateral side. But, as Fig. 8 shown a large shear stress develops at sections close to the right lateral side, and the magnitude gradually decreases as the value x/b moves toward zero. Likewise the longitudinal and lateral stresses the sear stress is nonzero when $x/b = 0.0$.

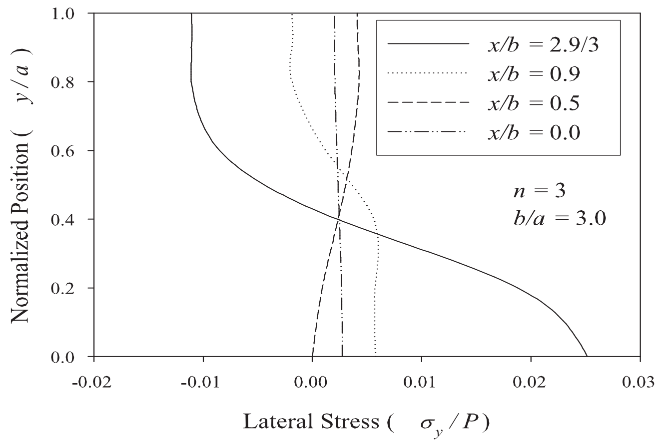

FIGURE 7. Lateral stress at different sections of the panel

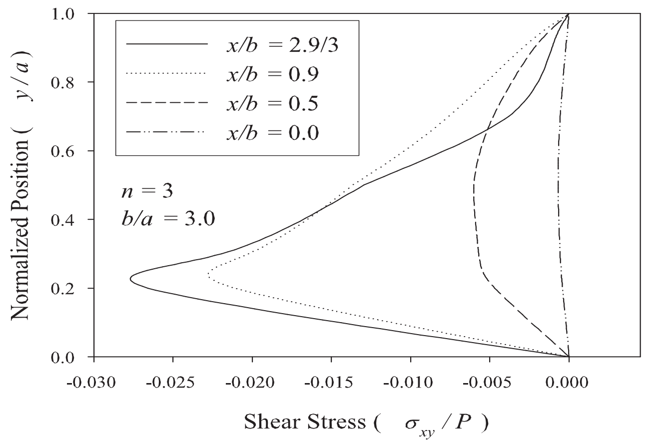

FIGURE 8. Shear stress at different sections of the panel

4. CONCLUSIONS

A symmetric cross-ply laminated composite material has been investigated based on the displacement potential approach for an orthotropic lamina. The formulation developed in the present study can be used for all types of the boundary conditions which are prescribed in terms of stress, or displacement, or mixed. A panel of glass/epoxy laminated composite is adopted to justifies the validity of the developed formulation. The results confirm that useful information about the actual stress and displacement at the critical regions of constraints and loadings can be obtained through the displacement potential approach. Therefore, the solutions obtained can be applicable to analyze elastic field in structural elements of laminated composite, and will be helpful to understand the behaviors of elastic laminated composite materials.

ACKNOWLEDGEMENT

The authors of this paper were partly supported by the Second Stage of Brain Korea21 Projects.

REFERENCES

[1] Afsar A.M., Huq N.M.L., and Song J.I.(2010)Analytical solution to a mixed boundary value elastic problem of a roller-guided panel of laminated composite. Arch. Appl. Mech., 80:401-412.

[2] Afsar A.M., Nath S.K.D., and Ahmed S.R.(2008) Displacement potential based finite difference solution of orthotropic composite beam under uniformly distributed and point loadings. Mech. Adv. Mater. Struct., 15(5):386 $\sim$ 399.

[3] Ahemd S.R., Idris A.B.M., and Uddin M.W.(1999) An alternative method for numerical solution of mixed boundary-value elastic problems. J. Wave-Mater. Interaction, 14(1-2):12-25.

[4] Chow L., Conway H.D., and Winter G.(1952) Stresses in deep bars. Trans ASCE 2557.

[5] Conway H.D.and Ithaca N.Y.(1953) Some problems of orthotropic plane stress. J. App. Mech., Trans ASME 52:72-76.

[6] Nath S.K.D., Afsar A.M., and Ahmed S.R.(2007a) Displacement potential approach to solution of stiffened orthotropic composite panels under uniaxial tensile load. J. Aero. Eng., IMechE., Part G, 221:869-881.

[7] Nath S.K.D., Afsar A.M., and Ahmed S.R.(2007b) Displacement potential solution of a deep stiffened cantilever beam of orthotropic composite material. J. Strain Analysis IMechE, 42(7):529 $\sim$ 541.

[8] Timoshenko S. and Goodier V.N.(1979) Theory of Elasticity. McGraw-Hill, New York.

[9] Uddin M.W.(1966) Finite Difference Solution of Two-dimensional Elastic Problem with Mixed Boundary Conditions. M. Sc. Thesis, Carleton University, Canada.

[10] Jones R.M.(1975) Mechanics of Composite Materials. 1^{st} ed., Scripta Book Company, Washington, D.C.